



Depósito de Investigación
Universidad de Sevilla

Depósito de investigación de la Universidad de Sevilla

<https://idus.us.es/>

“This is an Accepted Manuscript of an article published by Elsevier in INTERNATIONAL JOURNAL OF BIOLOGICAL MACROMOLECULES on 2020, available at: <https://doi.org/10.1016/j.ijbiomac.2020.10.006>”

1 Biodegradable doubly cross-linked chitosan hydrogels as
2 sustained drug delivery systems. Influence of chemical cross-
3 linking and chitosan ratios on rheological properties and
4 pharmacological performance.

5 *Nieves Iglesias¹, Elsa Galbis¹, Concepción Valencia^{2,3}, M. Jesús Díaz-Blanco^{2,3}, Bertrand*
6 *Lacroix^{4,5}, M.-Violante de-Paz^{1,*}*

7 1. Departamento de Química Orgánica y Farmacéutica, Facultad de Farmacia,
8 Universidad de Sevilla, 41012 Sevilla, Spain

9 2. Departamento de Ingeniería Química, Campus de “El Carmen”, Universidad de
10 Huelva, 21071 Huelva, Spain

11 3. Pro2TecS—Chemical Process and Product Technology Research Center, Universidad
12 de Huelva, 21071 Huelva, Spain

13 4. Department of Materials Science and Metallurgical Engineering, and Inorganic
14 Chemistry, University of Cádiz, Cádiz, Spain.

15 5. IMEYMAT, Institute of Research on Electron Microscopy and Materials of the
16 University of Cádiz, Cádiz, Spain.

17 *Correspondence: vdepaz@us.es; Tel.: +34-954-556-740

18

19 Abstract

20 This study investigates the impact of dual ionic and covalent cross-links (ion-XrL and
21 cov-XrL) on the properties of chitosan-based (CTS) hydrogels as eco-friendly drug
22 delivery systems (DDS) for the model drug diclofenac sodium (DCNa). Citric acid and a
23 diiodo-trehalose derivative (ITrh) were the chosen ionic and covalent cross-linker,
24 respectively. The novel hydrogels completely disintegrated within 96 h by means of a
25 hydrolysis process mediated by the enzyme trehalase. As far as the authors are aware,
26 this is the first time that a trehalose derivative has been used as a covalent cross-linker
27 in the formation of biodegradable hydrogels. The impact of CTS concentration and
28 degree of cov-XrL on rheological parameters were examined by means of an
29 experimental model design and marked differences were found between the materials.
30 Hydrogels with maximum elastic properties were achieved at high CTS concentrations
31 and high degrees of cov-XrL. DCNa-loaded formulations displayed well-controlled drug-
32 release profiles strongly dependent on formulation composition (from 17% to 40% in 72
33 h). Surprisingly, higher degrees of covalent cross-linking led to a boost in drug release.
34 The formulations presented herein provides a simple and straightforward pathway to
35 design fully biodegradable, tailor-made controlled drug delivery systems with improved
36 rheological properties.

37 Keywords:

38 Ionic cross-linking; chemical cross-linking; controlled drug release; biodegradable; eco-
39 friendly formulations; viscoelastic hydrogels.

40 1. Introduction

41 Hydrogels constitute a group of polymeric materials that swell and retain a significant
42 fraction of water within their three-dimensional (3D). They exhibit tunable mechanical
43 properties, biocompatibility and biodegradability and are therefore widely applied in
44 biomedical and pharmaceutical fields: cell proliferation and differentiation [1], tissue
45 engineering and regenerative medicines [2,3], and wound dressing [4,5], among others.
46 However, one of their most promising uses is as a constituent of matrices for the
47 controlled release of bioactive molecules, [6,7]. For hydrogel applications as drug
48 delivery systems (DDS), their original 3D structure must be mechanically strong so that
49 they do not erode prematurely, and thus early release or diffusion of the drug to non-
50 target tissues is prevented. This would dramatically improve their therapeutic efficacy
51 and reduce drug-associated side effects [8]. Moreover, it is necessary their
52 disintegration under physiological conditions, preferably in harmless products to ensure
53 a good biocompatibility of the hydrogel [9].

54 Although hydrogels made from natural polymers may not provide sufficient mechanical
55 properties, they do offer their inherent biocompatibility as an advantageous property
56 [10]. Therefore, strengthen the natural-based hydrogel system while maintaining its
57 swelling, flexibility and degradability properties is pursued. Among the natural occurring
58 polymers, chitosan (CTS) is drawing the attention of the scientific community, in
59 particular, in biomedical applications because of its interesting biopharmaceutical
60 characteristics, well documented biocompatibility and low toxicity [11]. CTS is also able
61 to adhere to the mucosal surfaces within the body [8] and has demonstrated its capacity
62 to open tight junctions between epithelial cells though well-organized epithelia [12]
63 acting as a permeation enhancer.

64 An interesting review provides an overview of traditionally used and recently developed
65 methods for preparation and modification of chitosan-based hydrogels [13]. In general,
66 crosslinkers serve as a bridge linking different or the same polymer chains, forming a 3D
67 network, improving the mechanical strength and chemical stability in acidic solutions.
68 CTS hydrogels have been prepared via ionotropic gelation (ionic cross-linking) [2,14–18]

69 coordination with metal ions [19], and irreversible/covalent cross-linking between CTS
70 and the cross-linker [7,20–22], among others. Among the covalent stabilization
71 mechanism, one of the most widely used is the formation of imine bonds between
72 amino groups from CTS and the aldehyde groups from the cross-linker [8,23,24].

73 Although non-covalent cross-linked hydrogels show unique mechanical properties,
74 including both stiffness/toughness and elasticity/flexibility to retain the hydrogel
75 structure, most of them are mechanically weak and prone to fracture, greatly restricting
76 their applications [25]. Conversely, and regarding drug release, the reversible nature of
77 ionically cross-linked networks is useful since, once release in the drug in the medium
78 has been achieved, the formulations can subsequently disintegrate into biocompatible
79 components that then will be metabolized and eliminated from the body [26].

80 Different approaches can be followed to overcome the instability of ionotropic
81 hydrogels. Thus, for example; to improve the mechanical properties of ionically cross-
82 linked calcium-alginate hydrogels under physiological conditions, the formation of
83 interpenetrating polymer network was successfully conducted by Zhao *et al.* [27]. On
84 the other hand, covalent cross-linking can improve the mechanical properties of the
85 hydrogels [28] and consequently, dual covalent and ionic bonds can be considered as an
86 effective method to enhance the properties of CTS-based materials. However, only few
87 examples of dual cross-linking methods have been published. Zhuang *et al.* reported the
88 formation of CTS films through the utilization of citric acid as a dual ionic and covalent
89 linker [29]. Ionic and covalent cross-linking of CTS with CaSO_4 and genipin, respectively,
90 has also been investigated [30]. Additionally, cross-linked iminoboronate-CTS hydrogels
91 have also been reported in which boronate-based coordination and covalent cross-
92 linking occur [31]. On the other hand, when chemical cross-linking is involved, a
93 decrease in degradability is usually observed [28]. Labile bonds need being introduced
94 in the gels so that the former can be broken under physiological conditions. Thus,
95 ensuring the presence of labile covalent bonds in the chemical structure of the covalent
96 cross-linkers is a good strategy to overcome this drawback. Among the breakable
97 covalent bonds, glycosidic linkages are present in di-, oligo- or polysaccharides. They are
98 easily hydrolyzed by living systems by means of reactions catalyzed by extremely

99 common non-specific and specific glycosidase enzymes {also called glycoside
100 hydrolases, [32,33]}, such as cellulase, amylase, mannosidase, lactase and trehalase,
101 among others.

102 In this work, we aim to manufacture a set of biodegradable and eco-friendly chitosan-
103 based hydrogels with enhanced rheological properties as DDS by means of a double
104 cross-linking process. Sodium diclofenac (DCNa), one of the most frequently used non-
105 steroidal anti-inflammatory drugs (NSAID) was the model drug of choice. The hydrogels
106 were ionically and covalently cross-linked. The chosen covalent cross-linker was the
107 2,3,4,2',3',4'-hexa-*O*-acetyl-6,6'-diiodo-6,6'-dideoxy- α -D-Glucopyranosyl- α -D-
108 glucopyranoside (ITrh), a dielectrophilic derivative from the disaccharide α,α' -trehalose,
109 that bears a labile acetal group in its structure. As ionic cross-linker, citric acid (CA) was
110 the polyprotic acid of choice since it presents excellent antimicrobial and antioxidant
111 properties as well as excellent biocompatibility [29,34]. The chemical structure,
112 biodegradability under physiological conditions, thermogravimetric properties and
113 morphologies of the hydrogels were evaluated. Two parameters, CTS concentration and
114 degree of covalent cross-linking, were investigated to find the influence they exerted
115 not only on the physicochemical and rheological properties of the hydrogels prepared
116 based on CTS, but also on the release profiles of DCNa. Drug release tests under
117 physiological conditions were conducted to demonstrate the in vitro controlled drug
118 release of DCNa. The prepared CTS-based hydrogels have demonstrated to be fully
119 biodegradable and endowed with controlled DCNa release properties under
120 physiological conditions for advanced therapies in which dual ionic and covalent cross-
121 links were involved. As far as the authors are aware, this is the first time that a trehalose
122 derivative has been used as a biodegradable covalent cross-linker in the formation of
123 structured polymeric materials.

124 2. Materials and methods

125 2.1. Materials

126 All the chemicals used were purchased from Sigma-Aldrich (Madrid, Spain) and used as
127 received. The phosphate buffer solution of pH 5.5 (25 °C) used for release assays was

128 freshly prepared when required. Chitosan (CTS) from Sigma-Aldrich, with a
129 deacetylation degree of 75% was chosen. The molecular weight of the CTS was
130 determined by viscometric analysis. Its viscosity was measured in a buffered solution of
131 0.5 M acetic acid - 0.5 M sodium acetate solution at 25.0 ± 0.1 °C using an Anton Paar
132 AMVn automated microviscometer. The viscometric constants “a” and “K” in the Mark-
133 Houwink equation were previously determined for this solvent – CTS system and found
134 to be $a = 0.59$ and $K = 0.119 \text{ cm}^3 \text{ g}^{-1}$. The weight of the CTS used was calculated by means
135 of the Mark-Houwink equation ($[\eta] = 3.385 \text{ dL/g}$) and its value was 299 kDa. The
136 di-iodinated trehalose (ITrh) employed for covalent crosslinking (cov-XrL) was prepared
137 following the recipe described in Section 2.2.2. Trehalase (from porcine kidney, 1UN/0.5
138 mL) was supplied by Sigma–Aldrich, Spain.

139 Dialysis tubing cellulose membranes avg. flat width 25 mm (Mw 8,000-14,000) were
140 purchased from Sigma-Aldrich. Before the release, it was necessary to activate the
141 cellulose membrane of the dialysis tube following this procedure: washing the tubing in
142 water for 3 h, treating the tubing with a 0.3% (w/v) solution of sodium sulfide at 80 °C
143 for 1 min. Subsequently it was washed with water at 60 °C for 2 min and with a 0.2%
144 (v/v) solution of sulfuric acid. Finally, it was washed with hot water the acid.

145 2.2. Methods

146 2.2.1. General Methods

147 Fourier Transform Infrared (FTIR) spectra were recorded on a Jasco FT/IR 4200
148 spectrometer (Great Dunmow, Essex, UK) equipped with attenuated total single
149 reflection (ATR) accessory in the wavenumber range from 4000 to 400 cm^{-1} . Nuclear
150 magnetic resonance (NMR) and mass spectra were recorded at the CITIUS Service
151 (University of Seville). ^1H and ^{13}C NMR spectra were recorded at 300 K with a Bruker
152 AMX-500 for solutions in CDCl_3 . Chemical shifts (δ) are reported as parts per million
153 downfield from Me_4Si and J in Hz. J is assigned and not repeated. All the assignments
154 were confirmed by COSY and HSQC experiments. Mass spectra were obtained using a
155 Kratos MS80RFA instrument. High resolution mass spectra were recorded on a Q-
156 Exactive spectrometer.

157 2.2.2. Synthesis of 2,3,4,2',3',4'-Hexa-*O*-acetyl-6,6'-diiodo-6,6'-dideoxy- α -D-
158 Glucopyranosyl- α -D-glucopyranoside (ITrh)

159 The title compound was prepared according to a modified method of the procedure
160 followed by Sizovs *et al.* [35]. A suspension of iodine (22.23 g, 87.6 mmol) in dry
161 dimethylformamide (DMF, 200 mL) was prepared in round-bottom flask. A solution of
162 triphenylphosphine (24.20 g, 92.27 mmol) in dry tetrahydrofuran (THF, 38 mL) was
163 added to the iodine suspension followed by anhydrous trehalose (10 g, 29.2 mmol). The
164 reaction was allowed to proceed at 80 °C for 12 h and the solvents were removed under
165 reduced pressure. The resulting syrup was dissolved in methanol (250 mL) and basified
166 to pH 9 by means of sodium methoxide. The mixture was stirred for 2 h at r.t. and then
167 neutralized by the addition of the acidic resin DOWEX-2H (H⁺ form). Methanol was
168 removed under reduced pressure to yield a colored oil that was poured into water (150
169 mL). To facilitate the precipitation of the formed triphenylphosphine oxide, the aqueous
170 solution was stored at 4 °C for 24 h. A white solid appeared at the bottom of the flask
171 and the suspension was then filtered and washed with dichloromethane (DCM, 2 x 50
172 mL). The water from the aqueous solution was mostly removed under reduced pressure,
173 and the obtained oil was dried at high vacuum for 48 h in the presence of P₂O₅. The dry
174 oil was dissolved in dry pyridine (Py, 200 mL) and the solution was placed in an ice-bath.
175 Acetic anhydride (38 mL, 403 mmol) was slowly added and the reaction was allowed to
176 stir at 25 °C for 12 h. The reaction mixture was poured on ice, and then extracted with
177 dichloromethane (DCM, 4 x 50 mL). The combined organic layers were washed with a
178 dilute solution of sulfuric acid and dried over Na₂SO₄. Na₂SO₄ was filtered off and the
179 solvent removed under reduced pressure yielding a yellowish oil. The product was
180 purified by column chromatography (eluent gradient: from 1:1 *tert*-butyl methyl ether-
181 hexane to 1:4 *tert*-butyl methyl ether-hexane) to yield the title compound (23.2 g,
182 25.0%). The ITrh spectra are recorded in Figures S1 to S4 in Supplementary information.

183 ¹H-NMR (500 MHz, CDCl₃) δ ppm: 5.55 – 5.46 (m, 2H, H-3), 5.42 (d, 2H, H-1, $J_{1,2}$ = 4.0 Hz),
184 5.19 (dd, 2H, H-2, $J_{2,3}$ = 10.5 Hz), 4.91 – 4.86 (m, 2H, H-4), 3.95 (dt, 2H, H-5, $J_{5,6a}$ = 2.5 Hz;
185 $J_{4,5}$ = $J_{5,6b}$ = 9.5 Hz), 3.23 (dd, 2H, H-6a, $J_{6a,6b}$ = 11.0 Hz), 3.06 (dd, 2H, H-6b), 2.14, 2.07.
186 2.02 (3 s, 19 H, 6 methyl groups). ¹³C-NMR (125 MHz, CDCl₃) δ ppm: 169.92, 169.59,

187 169.46 (carbonyl groups from acetyl moieties), 91.78 (C-1), 72.35 (C-4), 69.96, 69.76,
188 69.31 (C-5, C-3, C-2), 21.17, 20.68, 20.62 (methyl groups), 2.44 (C-6). IR: ν_{\max} (cm⁻¹) 1742,
189 1367, 1216, 1028, 656, 593, 566, 558, 528, 513, 493. ESI-MS positive ion mode:
190 calculated m/z (C₂₄H₃₂O₁₅I₂Na)⁺ ([M+Na]⁺): 836.9723; found m/z: 836.9721; $\Delta(m/z)$:-
191 0.2498 ppm.

192 2.2.3. Preparation of Hydrogels from Cross-linked Chitosan (CTS), Citric Acid (CA)
193 and Diiodinated Trehalose derivative (CTS_x-CA₁₀-ITrh_y)

194 Ten systems named CTS_x-CA₁₀-ITrh_y were prepared according to the procedure
195 described below (Figure S5). The targeted final CTS concentrations in mass percentages
196 (weight/weight or w/w) were 3%, 4% or 5% w/w and the degree of ionic cross-linking
197 (ion-XrL) was fixed by 10% for all the samples. Finally, the degree of cov-XrL was set at
198 0%, 5% or 10%. In Table 1 and along the text “x” denotes CTS concentration (% w/w),
199 and “y” denotes the degree of cov-XrL in the hydrogel. The ionic cross-linker was added
200 dissolved in double-distilled water (10 mg/mL concentration), the covalent cross-linker
201 was added in ethanol (50 mg/mL concentration) at 40 °C, and the final mass was
202 adjusted to 25 g with double-distilled water.

203 The general procedure followed for the preparation of aqueous cross-linked CTS-CA-ITrh
204 conjugates is summarized next (Figure 1, Table S1) and, as an example, the recipe
205 includes the amounts of the reagents necessary for the preparation of sample
206 CTS₄-CA₁₀-ITrh₅ (hydrogel with 4% w/w polymer concentration, 10% of degree of ion-XrL
207 and 5% of degree of cov-XrL): CTS with a deacetylation degree of 75% (CTS, 1 g, 4.36
208 mmol of free amine groups) was charged in a flask provided with a stirrer bar; then, an
209 aqueous solution of citric acid (CA, 2.80 mL, 1% w/v, 0.15 mmol), a solution of
210 di-iodinated trehalose derivative in ethanol (ITrh, 1.78 mL, 5% w/v, 0.11 mmol), a
211 solution of acetic acid (HAc, 0.25 mL, 52% w/v) and double-distilled water (up to a final
212 weight of 25 g, and final polymer concentration of 4% w/w) were added in sequence.
213 Five-minute stirrings were performed between the addition of each reagent. Once all
214 the reagents were added, the mixture was stirred for another 90 min at 40 °C. The
215 solution was cooled to room temperature, the stir bar removed, and stirring proceeded

216 overnight on a roller at 25 °C. The gelation of the systems was confirmed when the
 217 mixtures stopped flowing upon tube inversion for 60 s [23] (Figure S5). Three different
 218 batches of these conjugates were synthesized for comparative purposes.

219 **Table 1.** CTS concentration and degree of covalent cross-linking of the 10 CTS-based hydrogels
 220 prepared. Rheological parameters.

Sample	Formulation code	CTS Conc. (%w/w)	Degree cov-Xr (%)	pH	Rheological properties ^a				
					Tan δ (at 1 rad/s)	G' ₁ (Pa)	m	K (Pa·s ⁿ)	n
1	CTS ₃ -CA ₁₀ -ITrh ₀	3%	0	5.6	1.58	10.4	0.70	65.68	0.46
2	CTS ₃ -CA ₁₀ -ITrh ₅	3%	5	5.6	1.50	17.2	0.63	43.68	0.50
3	CTS ₃ -CA ₁₀ -ITrh ₁₀	3%	10	5.5	1.14	30.7	0.61	61.67	0.50
4	CTS ₄ -CA ₁₀ -ITrh ₀	4%	0	5.8	0.87	73.3	0.46	233.97	0.31
5	CTS ₄ -CA ₁₀ -ITrh ₅	4%	5	5.5	0.84	121.5	0.42	237.54	0.30
6	CTS ₄ -CA ₁₀ -ITrh ₅	4%	5	5.9	0.77	93.1	0.45	251.33	0.30
7	CTS ₄ -CA ₁₀ -ITrh ₁₀	4%	10	5.3	0.70	146.0	0.39	324.39	0.22
8	CTS ₅ -CA ₁₀ -ITrh ₀	5%	0	6.3	0.68	233.9	0.39	475.41	0.18
9	CTS ₅ -CA ₁₀ -ITrh ₅	5%	5	6.2	0.63	249.8	0.33	463.41	0.17
10	CTS ₅ -CA ₁₀ -ITrh ₁₀	5%	10	6.3	0.46	653.3	0.29	449.07	0.17

Degree of ionic cross-linking: 10% in every sample;

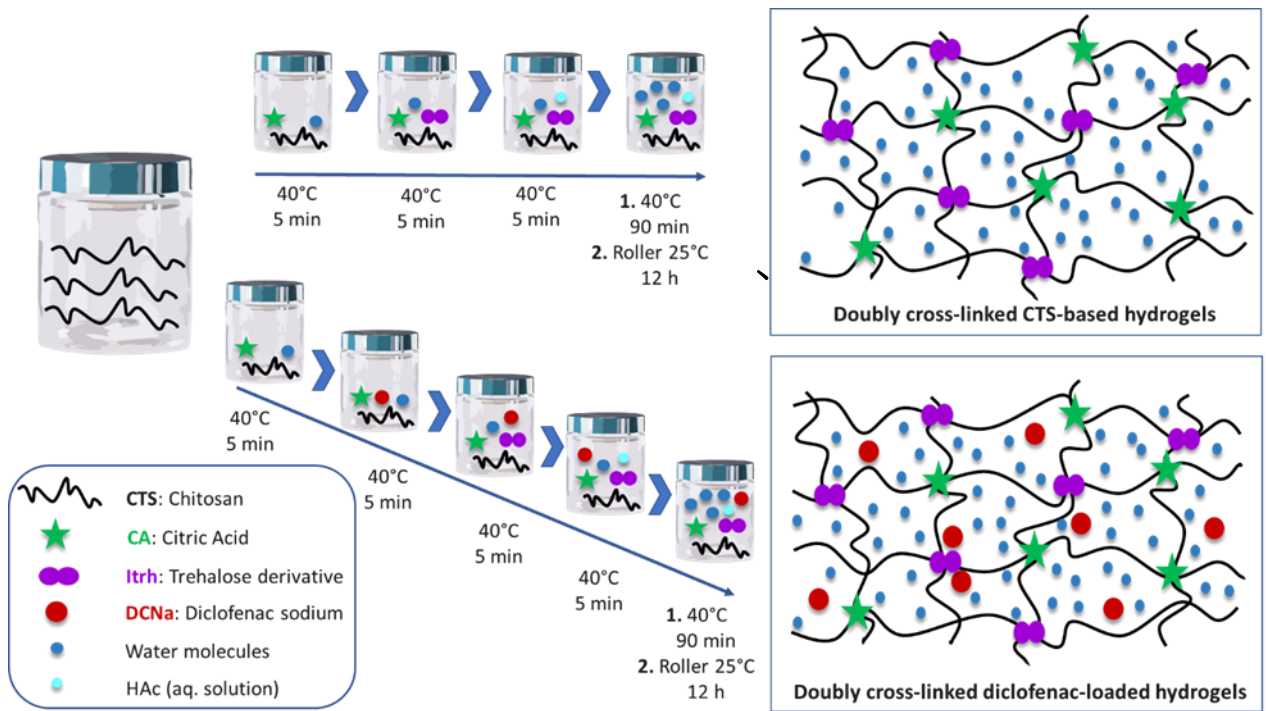
CTS conc = concentration (in w/w percentage) of CTS;

Degree cov-Xr = degree of covalently cross-linked amino groups in CTS material by diiodo trehalose derivative;

^aPower-law model parameters and loss tangent at 1 rad/s for CTS_x-CA₁₀-ITrh_y hydrogels studied.

221

222 **Figure 1.** General procedure for the formation of doubly cross-linked CTS-CA-IThr hydrogels.



2.2.4. Preparation of Diclofenac Sodium Loaded Formulations from Cross-linked Chitosan-Conjugates

Ten systems named DCNa-CTS_x-IThr_y were prepared. The preparation process was similar to that of non-loaded hydrogels except that a solution of DCNa in ethanol was added into the mixture just after the ionic cross-linker CA (Figure 1). Final CTS concentrations: 3%, 4% or 5% w/w; degree of ion-XrL: 10%; degree of cov-XrL: 0%, 5% or 10%; final DCNa concentration: 1% w/w.

2.2.5. Hydrogel studies

The dried samples were examined by thermogravimetric analysis (TGA), and the decomposition temperatures were observed. The thermogravimetric analyzer was TA Instruments Q-600 SDT (New Castle, DE, USA). Platinum pans containing approximately 5 mg of each sample were used. Trials were conducted under inert atmosphere (nitrogen, flow rate: 100 mL/min, heating rate: 10°C/min), from 0°C to 700°C.

237 To measure the pH of the samples, the selected hydrogel (1 g) was placed in a glass
238 container and 10 mL of double-distilled water was added. It was shaken gently and the
239 obtained pHs are shown in Table 1. pH readings of the samples were determined
240 electrometrically using digital pH-meter (HI98103; Hanna Checker pH-meter, Hanna
241 Instruments).

242 2.2.6. In vitro degradation of CTS_x-CA₁₀-ITR_{h_y} hydrogels

243 The in vitro degradation studies of hydrogels were conducted following the procedure
244 described by Liu and coworkers for collagen-based hydrogels [36]. Thus, 60-80 mg of
245 hydrated hydrogels (n = 3 of each formulation) were immersed in vials containing 5 mL
246 of 0.1 M PBS (pH 5.7), followed by addition of 30 µl trehalase (2UN/mL). The vials were
247 incubated at 37 °C with shaking at 100 rpm. At different time intervals, the hydrogels
248 were taken out and rinsed with double-distilled water to remove excess salinity. The
249 weight of each sample was measured after all surface water was carefully blotted off.
250 The percent residual mass of hydrogels was calculated according to Equation 1:

$$251 \quad \text{Residual mass (\%)} = \frac{W_t}{W_0} \times 100 \quad (\text{Eq. 1})$$

252 where W_0 is the initial weight of the hydrogel and W_t is the weight of the hydrogel at
253 each time point.)

254 2.2.7. Rheological Studies and Experimental

255 CTS_x-CA₁₀-ITR_{h_y} hydrogels were rheologically characterized in a controlled-strain (ARES,
256 Rheometric Scientific, Surrey, UK) rheometer, using a serrated plate-plate (25 mm
257 diameter, 1 mm gap) geometry. Small amplitude oscillatory shear (SAOS) tests were
258 carried out inside the linear viscoelastic region in a frequency range of 0.03–100 rad/s
259 at 25 °C. Strain sweep tests were previously performed to determine the linear
260 viscoelastic regime. Viscous flow tests were also made by applying a stepped shear rate
261 ramp in a shear rate range of 0.06–100 s⁻¹ at 25 °C. Each fresh sample was tested at least
262 in duplicate. The rheological parameters obtained are recorded in Table 1.

263 2.2.8. Experimental Model Design for the analysis of rheological parameters

264 In order to study the influence of CTS concentration and the degree of cov-XrL in the
265 rheological properties of the hydrogels, a Box–Behnken experimental design (CSS
266 Statistica, StatSoft Inc., Tulsa, UK) was used to evaluate the significance of these
267 independent variables as well as the interactions among them in the rheological
268 parameters G'_1 , m , $\tan \delta$, K and n . The number of experiments (N) is defined by the
269 Equation 2:

270
$$N = k^2 + k + cp \quad (\text{Eq. 2})$$

271 where k represents the number of factors (variables) involved in the study and cp is the
272 number of replicates of the central point. Box–Behnken could be seen as a cube,
273 consisting of a central point and the middle points of the edges.

274 The total number of experiments required for our considered independent variables at
275 three levels was 10. The values of the selected pair of independent variables were
276 normalized from -1 to +1 by using Equation 3 in order to facilitate direct comparison of
277 the coefficients and visualization of the effects of the individual independent variables
278 on the response variable.

279
$$X_n = \frac{X - \bar{X}}{(X_{max} - X_{min})/2} \quad (\text{Eq. 3})$$

280 where X_n is the normalized value of independent variables; X is the absolute
281 experimental value of the variable concerned; \bar{X} is the mean of all fixed values for the
282 variable in question; and X_{max} and X_{min} are the maximum and minimum values of the
283 variable, respectively.

284 2.2.9. Diclofenac Sodium Release Studies

285 The evaluation of drug release was conducted by ultraviolet-visible (UV-vis)
286 spectroscopy. UV-vis measurements of DCNa-loaded hydrogels were performed with a

287 Shimadzu UV-2102 PC UV–visible spectrophotometer (Kyoto, Japan). The data were the
288 result of, at least, three measurements.

289 Prior to the release analyses, a calibration curve of DCNa concentration against
290 absorbance at 280 nm was made with six DCNa standard solutions (buffered solutions
291 at pH 5.5). The equation obtained (Equation 4) determines the linear relationship
292 between UV absorbance (A , at 280 nm) and DCNa concentration (C , in mg/mL) in the
293 range of drug concentration studied (from 100 $\mu\text{g/mL}$ to 12.5 $\mu\text{g/mL}$).

$$294 \qquad \qquad \qquad A = 27.525 C + 0.027 \qquad \qquad \qquad (\text{Eq. 4})$$

295 The selected hydrogel (1 g) was transferred to a dialysis tubing cellulose membrane
296 (molecular weight cut-off: 8,000–14,000 Da), then immersed in 200 mL of phosphate
297 buffer at pH 5.5 in a round-bottom flask provided with a stirrer bar at 37 °C. At pre-
298 designed time intervals, aliquots were taken from the release medium and the amount
299 of DCNa released was determined by UV–vis spectroscopy at 280 nm. One mL of pre-
300 heated buffer solution was added to the release medium to maintain a constant volume.
301 Experiments were performed in triplicates.

302 2.2.10. Studies of Hydrogels Morphologies by Scanning Electron Microscopy

303 The morphologies of selected samples were examined by Scanning Electron Microscopy
304 (SEM) using a field emission scanning electron microscope FEI Teneo. Images were
305 recorded at an accelerating voltage of 5 kV using secondary electrons. Before SEM
306 observations, the hydrogel scaffold was directly frozen at -20 °C for 3 h, then at -80 °C
307 for 24 h [37]. After that, the samples were lyophilized by freeze drying for 24 h. Small
308 pieces of dry hydrogels were cut by razors, then fixed on aluminum stubs using a double-
309 sided carbon tape and finally sputter-coated with about 20 nm of gold.

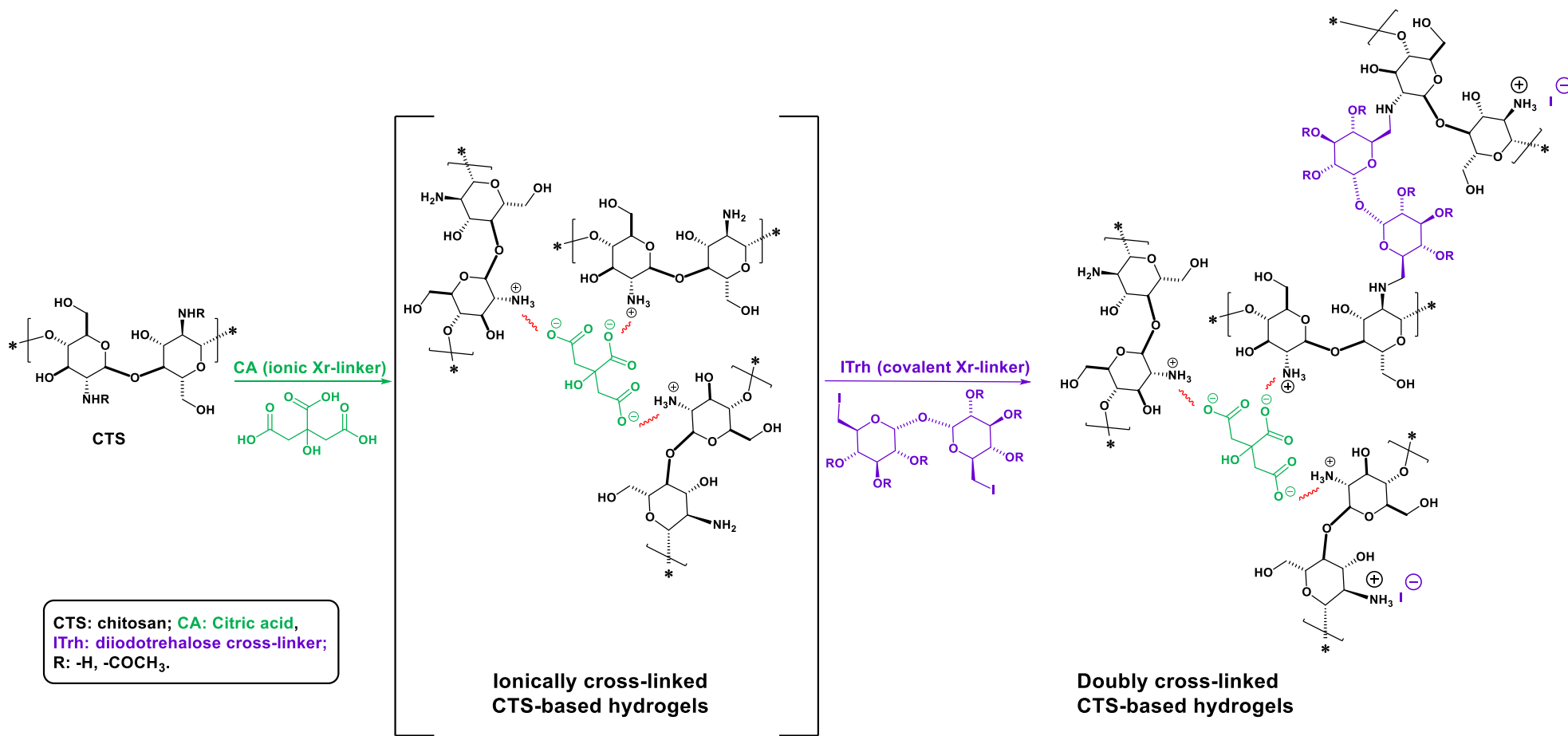
310 3. Results and discussion

311 In the present work we focused on the preparation of CTS-based hydrogels by combining
312 ion-XrL with cov-XrL in order to increase the viscoelastic properties of CTS hydrogels
313 regarding those recently found for ion-XrL hydrogels [17] and study their impact on the

314 transport of a model anionic API, DCNa. Another parameter to investigate was the effect
315 of an increment in CTS percentages regarding those tested in the previous study as well
316 as the use of another ionic cross-linking agent, CA, which could also enhance hydrogen
317 bonds formation in the hydrogel structure. The impact of this double cross-linking on
318 the release kinetics of the anionic drug will be addressed.

319 3.1. Preparation of Hydrogels from Cross-linked Chitosan (CTS), Citric Acid 320 (CA) and Diiodinated Trehalose (ITrh) (CTS_x-CA₁₀-ITrh_y)

321 The tricarboxylic ionic cross-linker CA and the electrophile (and covalent cross-linker)
322 derived from α -D-trehalose, the 6,6'-dideoxy-2,3,4,2',3',4'-hexa-O-acetyl-6,6'-diiodo- α -
323 D-glucopyranosyl- α -D-glucopyranoside (ITrh), were used to render a new family of
324 doubly-cross-linked hydrogels. The ionic cross-linking agent, CA, allowed the
325 establishment of ionic bonds and hydrogen bonding with the ionized amine groups and
326 the hydroxyl groups from CTS. The cross-linker ITrh, a disaccharide with hydrolyzable
327 glycosidic bond in its structure, was used in aqueous media. This cross-linking agent
328 reacted with the amino groups of the CTS leading to 3D networks, with potential
329 degradable properties under physiological conditions (Scheme 1).



330

331 **Scheme 1.** Reactions involved in the formation of doubly cross-linked CTS-CA-IThr hydrogels.

332 ITrh was synthesized by a modified procedure from Sizovs *et al.* [35]. Due to the
333 symmetrical character of the starting disaccharide material α,α -trehalose, the two
334 iodine groups at C-6 and C-6' could be considered equivalent, and a double reaction with
335 amine groups from CTS was likely to occur.

336 ^1H NMR, COSY ^1H NMR, ^{13}C NMR and ESI-MS of the diiodo derivative from α -D-trehalose
337 (ITrh) are recorded in Figures S1-S4. Due to the symmetry of the molecule, NMR spectra
338 —mono and two-dimensional $^1\text{H},^{13}\text{C}$ and COSY— do not show high complexity. Spectral
339 analyses confirmed the chemical structure of the cross-linker. Thus, the presence of two
340 double doublets at *ca.* 3.2 and 3.1 ppm in the ^1H MNR and COSY spectra, correlated to
341 the protons from the iodomethylene units of the glucopyranose rings, should be stood
342 out. It is also noteworthy the presence of a peak at 2.5 ppm in the ^{13}C NMR spectrum
343 associated to the mentioned methylene groups. Moreover, the chemical structure of
344 ITrh was unequivocally confirmed by its Electrospray Ionization (ESI) High Resolution
345 mass spectrum, with a peak at *m/z* ratio 836.9721, corresponding to $[\text{M}+\text{Na}]^+$ ion.

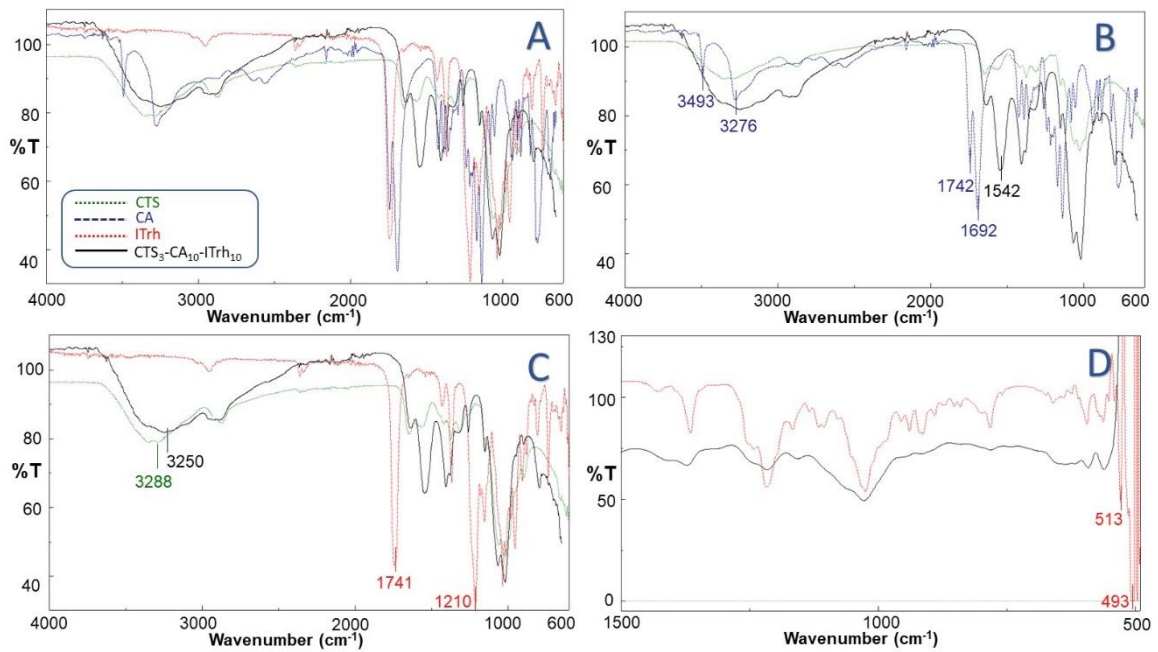
346 To confirm the cross-linking in the hydrogels, FTIR spectra of the starting materials and
347 the hydrogels were obtained (Figure 2). Figure 2A records the spectra of the polymer
348 (CTS), the two cross-linkers used (CA and ITrh) and one of the hydrogels formed (CTS₃-
349 CA₁₀-ITrh₁₀). In Figures 2B, 2C and 2D, only selected FTIR spectra and sections were
350 recorded.

351 The existence of ionic cross-linking interactions in CTS-based hydrogels was firstly
352 confirmed (Figure 2B). This ionic interaction occurred because of the acid-base reaction
353 between the carboxylic acid groups from CA and some of the amine groups from CTS. In
354 the CTS FTIR spectrum, O-H bonds from hydroxyl groups provide a broad band centered
355 at 3288 cm^{-1} , which is overlapped with the stretching bands corresponding to the N-H
356 bonds from amine and amide groups. In addition, several significant bands were of
357 interest in the FTIR spectrum of CA. The bands at 3493 and 3276 cm^{-1} (sharp and broad
358 bands, respectively) are mainly due to the stretching of the O-H bonds found in the
359 carboxylic acid groups of CA. Other two bands (1742 and 1692 cm^{-1}), both sharp and
360 intense, can be correlated to the stretching of C=O bonds present in the two types of

361 carboxylic acid groups of CA. None of these CA bands were present in sample 3
362 confirming the acid-base reaction mentioned above. In contrast, a new band at 1542
363 cm^{-1} (stretching band of C=O in carboxylate ions), has emerged as well as a shift of st
364 N-H band, (at 3250 cm^{-1}), in this case correlated with the freshly formed ammonium ions
365 from CTS protonation.

366 From the chemical point of view, the covalent cross-linking took place by a nucleophilic
367 reaction in which some amine groups of CTS attacked the iodomethylene moieties of
368 ITrh, giving rise to secondary amino groups and iodide ions (Scheme 1). To detect that
369 this cross-linking reaction was successfully accomplished, the disappearance of the
370 stretch band due to the covalent C-I bond in the ITrh cross-linker in the region
371 comprehended between 600 and 400 cm^{-1} was investigated. Figure 2D displayed the IR
372 of sample 3 and ITrh. As can be observed, the bands at 513 and 493 cm^{-1} associated to
373 the stretching of C-I bond [38] in unreacted ITrh were not found in the IR spectrum of
374 sample 3, which is the confirmation that the chemical cross-linking between CTS and
375 ITrh had taken place. It was also noticed that during the gelling procedure (Figure 2C),
376 the labile acetate groups from ITrh were hydrolyzed, as confirmed by the disappearance
377 of the bands at 1741 and 1210 cm^{-1} (stretching bands of C=O and O-CO bonds,
378 respectively).

379



380

381 **Figure 2.** FTIR spectra of CTS, the cross-linkers used (CA and ITrh) and one of the prepared
382 hydrogels freeze-dried (sample 3: CTS₃-CA₁₀-ITrh₁₀). The color code for Figures A, B C and D is as
383 follows: CTS: green; CA: blue; ITrh: red; CTS₃-CA₁₀-ITrh₁₀ hydrogel: black. Representative bands
384 have been included.

385 An experimental model design was conducted to study the influence of CTS
386 concentration and the degree of cov-XrL on the rheological properties of prepared
387 hydrogels. Ten systems named CTS_x-CA₁₀-ITrh_y, in which “x” denotes CTS concentration
388 (% w/w), and “y” denotes the degree of cov-XrL in the hydrogel, were prepared. The
389 targeted final CTS concentrations ranged from 3% to 5% w/w and the degree of cov-XrL
390 varied from 0%, to 10%), setting a degree of ion-XrL of 10% for all the trials (Table 1).

391 3.2. Thermogravimetric Analyses (TGA)

392 The thermal stability of the freeze-dried hydrogels was evaluated by thermogravimetry
393 under an inert atmosphere. Characteristic parameters resulting from the experiments
394 are provided in Table S2. Figure S6 displays the TGA curves of CTS, CA and Sample 3
395 (CTS₃-CA₁₀-ITrh₁₀).

396 The main peak of the thermograms was centered at values close to 300 °C and was
397 associated with the degradation of the cov-XrL ITrh and CTS backbone due to their

398 structural similarity. The thermo-degradation step centered at 215 °C and characteristic
399 for the ionic cross-linker CA was not observed in the thermograms of CTS-based
400 hydrogels. It could be inferred from this fact that CA is structurally integrated into the
401 hydrogel structures and is exerting its action as cross-linker effectively. This conclusion
402 is supported by the FTIR results already discussed.

403 On the other hand, and being all the samples highly hydrophilic materials, a weight loss
404 associated to water content was observed for all the formulations at low and high
405 temperatures. This was confirmed by the analyses of their thermograms: weight loss vs
406 temperature and non-reversible heat flow vs temperature plots. For both, CTS starting
407 material and hydrogel formulations, there was a clear endothermic event with
408 associated maximum weight loss in the range from 45 °C to 72 °C, probably due to water
409 molecules slightly attached to hydrogel structures [39]. It is remarkable that, after
410 experiencing the same freeze-dry procedure, that water content was substantially
411 higher in the freeze-dried hydrogels than that found in CTS, with increases in *ca.* 67%
412 (water content in CTS: 9%; water content in freeze-dried hydrogels: from 14 to 17%).

413 Moreover, in the case of hydrogel formulations, a bonus water content (from 7% to 13%)
414 was sustainably detached when heated to values close to 200 °C with maximum weight
415 losses at temperatures between 145 °C and 181 °C and depended on the concentration
416 of CTS: the higher the concentration of CTS, the lower their water content. However,
417 CTS itself showed no weight loss at temperatures ranging from *ca.* 120 °C to 220 °C. It is
418 hypothesized that water is firmly retained inside the 3D structure of the cross-linked
419 materials. Therefore, the new hydrogels possess enhanced water retention capacity
420 than may be closely related to the presence of more hydrophilic groups, such as -COO⁻,
421 -COOH, -NH₃⁺ and -OH, available as centers to attract water [40].

422 3.3. In vitro degradation of CTS_x-CA₁₀-ITRh_y Hydrogels

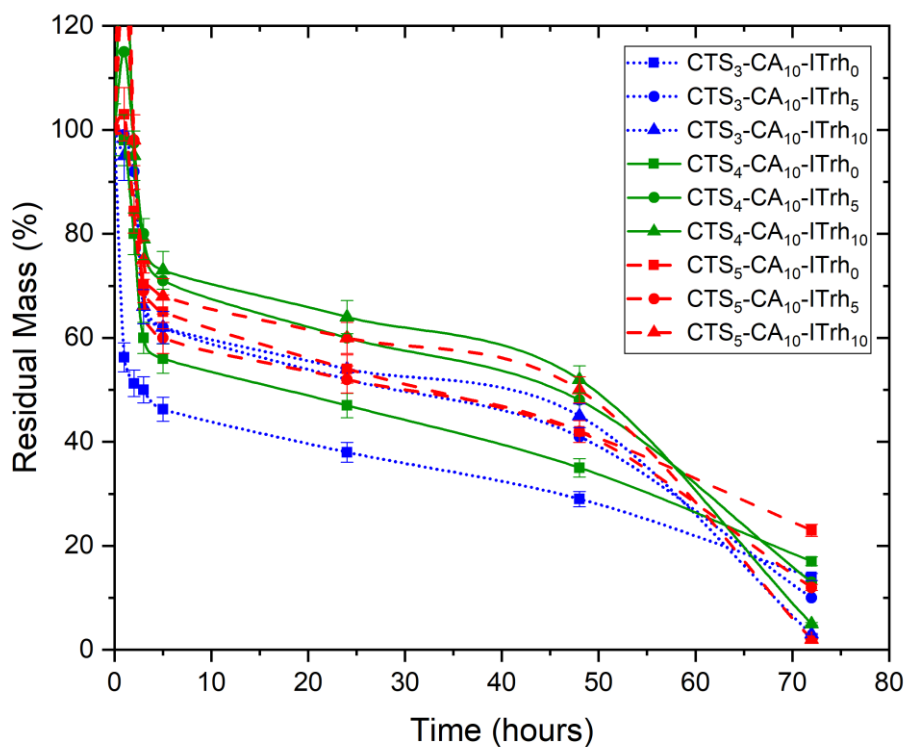
423 In general terms, in vitro degradation of polysaccharide-based hydrogels can occur in
424 the polymer backbone through a hydrolytic process that usually causes the breakage of
425 the glycosidic bonds of the polysaccharide chains [41]. In the case of CTS-based
426 hydrogels, hydrolysis takes place either in an acidic medium [42] or mediated by the
427 enzyme lysozyme [43]. Other options are breaking the cross-links and thereby releasing

428 the biocompatible polysaccharide. In this work, cross-links are the goal of degradation
429 experiments.

430 The in vitro degradation of the CTS-CA-ITrh hydrogels focused on the lysis of such
431 cross-links by hydrolytic procedures —mediated or not by thehalase— in an acidic
432 microenvironment (pH = 5.7). It was monitored the residual mass percentage of the
433 matrix as a function of time. The reversibility of ionic cross-linking in aqueous media has
434 been well established [25] and hence, a straightforward breakdown of the interactions
435 between CTS and CA was expected. The other cross-linking found in these hydrogels is
436 the trehalose bridges between the CTS chains that were formed during the gelling. These
437 bridges are expected to be degraded by the enzyme trehalase, responsible for the
438 catalytic hydrolysis of the acetal group of trehalose. Under these conditions, certain
439 degree of hydrolysis of the CTS backbone cannot be ruled out.

440 From the degradation trials, some the samples experienced a water gain in the first few
441 hours, mainly those with higher CTS content, and then a rapid mass loss was observed
442 (from 27 to 54%, depending on the system, Figure 3). This effect could be due to the
443 partial solubilization of the ionic cross-linker in the medium, with the concurrent water
444 loss, causing a loosening of the hydrogel structure. The slower weight loss rates
445 observed for higher cross-linked samples were in line with other authors' observations
446 for covalently cross-linked CTS-based hydrogels [23]. Quasi-plateau regions were
447 observed in the degradation profiles of covalent-cross-linked hydrogels, suggesting a
448 slowdown in their degradation patterns. This could be explained by the need for the
449 enzyme to diffuse into the already eroded hydrogel structure to exert its action.

450 In intermediate stages of the degradation processes, the most cross-linked systems
451 showed greater hydrolytic stability as demonstrated by Guo and collaborators in the
452 hydrolysis of injectable hydrogels prepared from chitosan-*graft*-polyalanine and
453 oxidized dextran as cross-linker [23]. However, as the degradation experiments
454 progressed, the degradation profiles resembled each other, all being fully disintegrated
455 within 96 h. Trehalose links have demonstrated to be biodegradable under physiological
456 conditions.



457

458 **Figure 3.** *In vitro* degradation patterns of CTS-CA-ITrh hydrogels conducted at pH 5.7 and 37 °C
 459 in the presence of trehalase. The inset shows the successful biodegradation of the samples under
 460 the experimental conditions. Error bar: standard deviation ($n = 3$ different samples for each
 461 formulation)

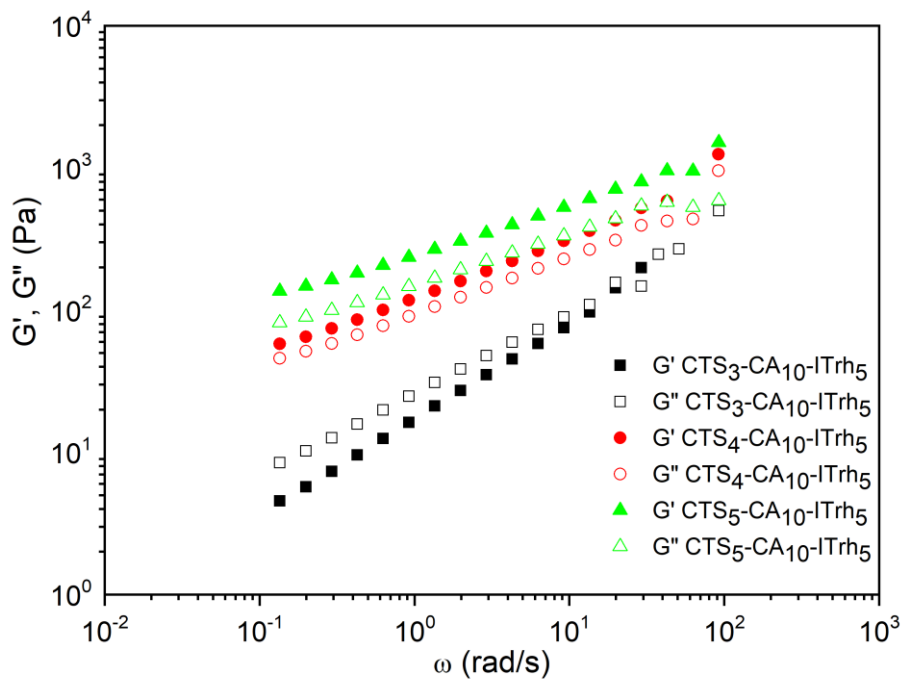
462

463 3.4. Rheological Characterization of CTS_x-CA₁₀-ITRh_y Hydrogels. Correlations
 464 of Rheological Parameters with CTS Concentration and Degree of
 465 Covalent Cross-linking Based on an Experimental Model Design

466 The ten hydrogels prepared were rheologically characterized. The influence of CTS
 467 concentration and the degree of cov-XrL on significant rheological parameters, such as
 468 elastic modulus G' , $\tan \delta$, consistency, K , and flow, n indexes were mathematically
 469 studied by means of Box Behnken experimental designs.

470 Figure 4 shows the evolution of the linear viscoelasticity functions, storage or elastic
 471 modulus (G') and loss or viscous modulus (G''), with frequency, as a function of CTS

472 concentration for samples with ionic degree XrL of 10% and cov-XrL of 5%. As can be
 473 observed, it was apparent that an increase in CTS concentration yielded larger figures
 474 for the linear viscoelasticity functions as has been demonstrated for other CTS-based
 475 hydrogels [20]. The G'' values were higher than those found for G' at low CTS
 476 concentration and a tendency to reach a crossover point between these functions was
 477 obtained at high frequencies. On the other hand, G' values were higher than G'' ones at
 478 higher CTS concentrations throughout the studied frequency range.



479
 480 **Figure 4.** Frequency dependence of the storage, G' , and loss, G'' , moduli at 25°C, in the linear
 481 viscoelasticity region, for hydrogels as a function of CTS concentration.

482 Aiming to quantify the dependence on CTS concentration and covalent cross-linked
 483 degree, a power-law equation (Equation 5) has been used to describe the evolution of
 484 the storage modulus, G' , with frequency:

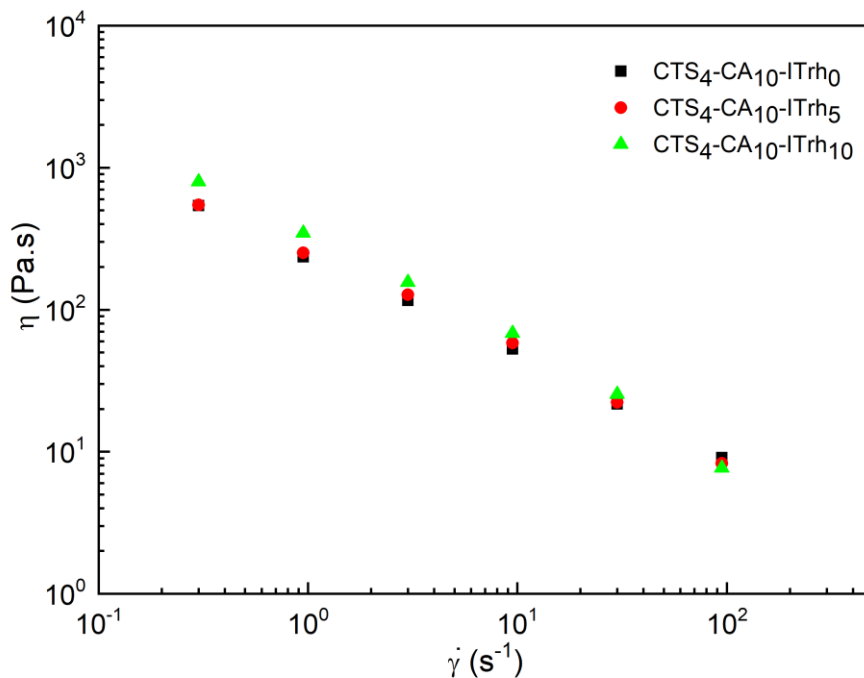
$$485 \quad G' = G'_1 \times \omega^m \quad (\text{Eq. 5})$$

486 where G'_1 and m are fitting parameters.

487 Figure 5 illustrates the viscous flow behavior exhibited by selected hydrogels as a
 488 function of the degree of cov-XrL. A shear-thinning behavior was apparent in all samples,
 489 which could be fitted well to the power-law model (Equation 6):

490
$$\eta = K \cdot \dot{\gamma}^{n-1} \quad (\text{Eq. 6})$$

491 where K and n are the consistency and flow indexes, respectively. The values of fitting
 492 parameters are shown in Table 1. As can be observed an increase in cov-XrL yielded
 493 higher viscosity values.



494
 495 **Figure 5.** Viscous flow curves for hydrogels, at 25°C, as a function of covalent cross-linked
 496 degree.

497 A Box–Behnken experimental design was used to evaluate the significance of these
 498 independent variables (CTS concentration and degree of cov-XrL) related to the
 499 rheological parameters recorded in Table 1. In general, for the dependent parameters
 500 evaluated in the intervals studied, a greater influence of CTS concentration was
 501 observed with respect to that found for the degree of cov-XrL.

502 In Table 2 the obtained equations by using polynomial regression and the calculated
 503 statistics parameters (R^2 , d_f and F) are shown. In this sense, a suitable (>0.97) R^2 and
 504 (>35) F values have been found in equations.

505 **Table 2.** Equations yielded for each dependent variable as a function of the independent
 506 variables (normalized values) for the Box-Behnken experimental design.

Equations	R^2	d_f	F
$\tan \delta = 0.838 - 0.41 [CTS] - 0.146 Xr + 0.218 [CTS]^2 - 0.08 Xr^2 + 0.055 [CTS] Xr$	0.994	5.4	146.32
$G'_1 (Pa) = 110.1 + 179.79 [CTS] + 113.8 Xr + 109.55 Xr^2 + 99.78 [CTS] Xr$	0.972	5.4	35.96
$m = 0.427 - 0.155 [CTS] - 0.0433 Xr + 0.064 [CTS]^2$	0.999	3.6	351.08
$K (Pa s^n) = 251.49 + 202.81 [CTS] + 7.87 Xr^2 - 5.58 [CTS] Xr$	0.999	3.6	712.65
$n = 0.30 - 0.1566 [CTS] + 0.03 [CTS]^2 - 0.0125 [CTS] Xr$	0.990	3.6	423.68

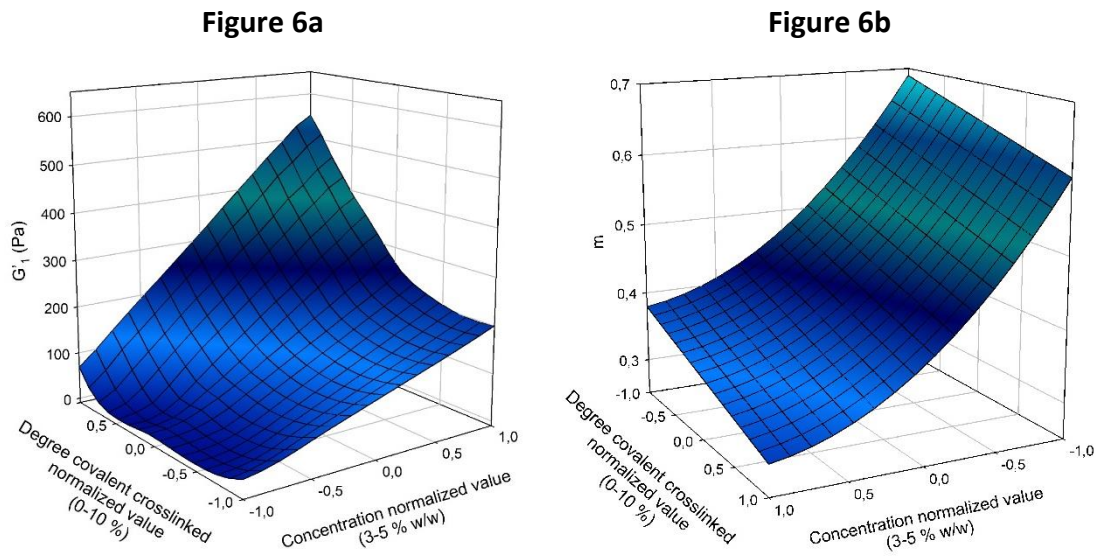
[CTS] = CTS concentration (% w/w), normalized value; Xr = degree of covalent cross-linking, normalized value; Tan δ = loss tangent (at 1 rad/s); G'_1 = storage modulus; m = power-law index; K (Pa s) = consistency index; n = flow index

507 To facilitate the identification, that on the selected dependent variable the independent
 508 variables are applied, the response surfaces for each dependent variable are shown in
 509 Figures 6, 7, S7a and S7b. In a set of hydrogels formed from chitosan-*graft*-polyaniline
 510 copolymer cross-linked with oxidized dextran, an increase in storage modulus was
 511 observed with the degree of cross-linking [23], similar to what was found for the
 512 hydrogels from this study, as shown below.

513 Figure 6a allows estimating the variation of G'_1 , with respect to cov-XrL and CTS
 514 concentration, over the range considered. These variations in G'_1 were more
 515 pronounced at the highest figures of the independent variables, *i.e.*, at 5% of CTS and
 516 10% of cov-XrL. Moreover, G'_1 was more sensitive to changes in polymer concentration
 517 than to the other independent variable. Thus, to obtain hydrogels with high G'_1 , it is
 518 advisable to operate with high degrees of cov—XrL and high CTS concentrations. On the
 519 contrary, the lowest values were found at medium-to-low degrees of cov-XrL and low

520 CTS concentrations. No significant G'_1 figures have been found at low concentrations.
521 These low G'_1 data were independent of the degree of cov-XrL.

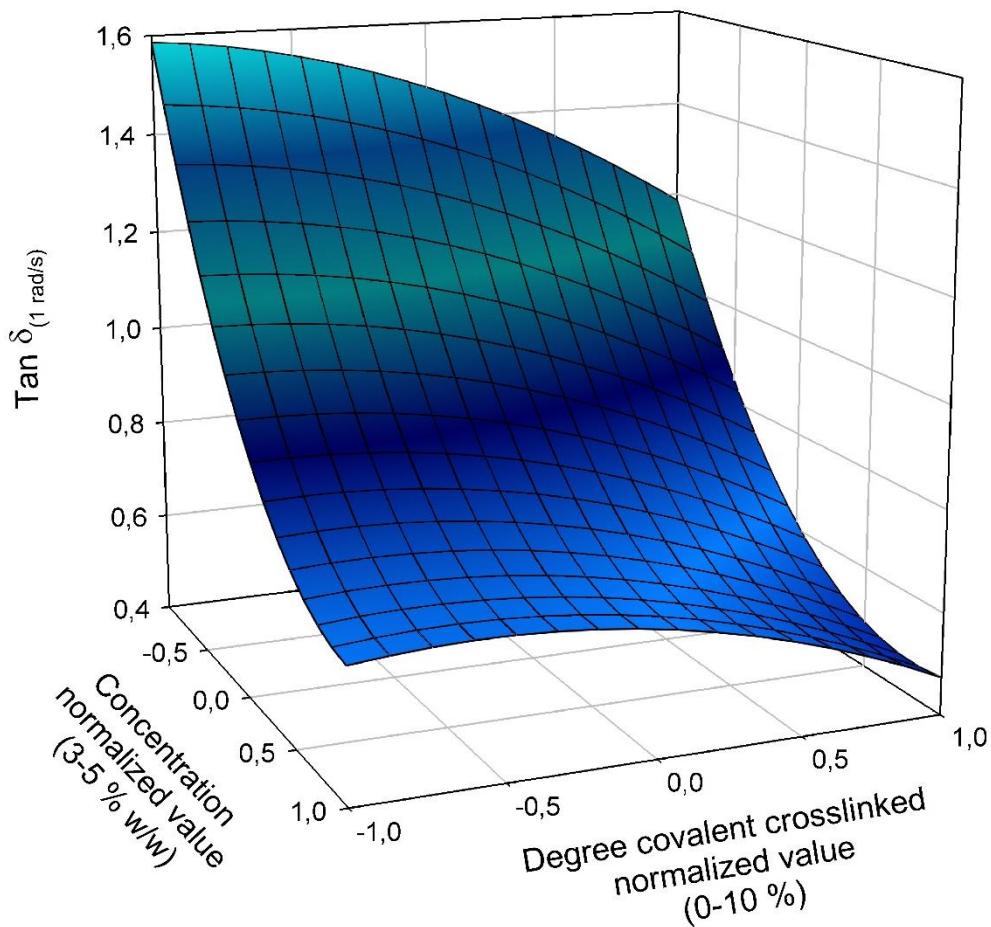
522 Similar to the findings regarding G'_1 , the percentage of cov-XrL displayed lower statistical
523 influence in the power-law index (m) (Figure 6b) than that exerted by CTS rates.
524 Moreover, a similar negative (lowered values) statistical influence for cov-XrL was found
525 under high and low CTS concentrations. In this way, the efficient selection of the
526 parameters studied entails the use of high CTS concentration and a high degree of
527 cov-XrL to obtain higher m values, fact that seems to indicate a more developed and
528 complex hydrogel microstructure.



529 **Figure 6.** Response surface models obtained from the Box–Behnken experimental design to
530 evaluate the relative influence of the independent variables (CTS concentration and degree of
531 cov-XrL) on the rheological parameters G'_1 (Fig. 6a) and m (Fig. 6b).

532 The response surface for the loss tangent ($\tan \delta = G''/G'$) is recorded in Figure 7 to
533 explore the relationships between the independent variables mentioned above and this
534 response variable. Thus, the statistical influences exerted by cov-XrL and CTS
535 concentration followed a similar trend as in the dependent parameters evaluated so far
536 (G'_1 , m). Thus, in order to achieve the lowest values for $\tan \delta$, the use of high CTS

537 concentrations and cov-XrL is advisable, indicating that, under these conditions, the
538 relative elastic properties of the hydrogels may increase.



539

540 **Figure 7.** Response surface model obtained from the Box–Behnken experimental design to
541 evaluate the relative influence of the independent variables (CTS concentration and degree of
542 cov-XrL) on the rheological parameter $\tan \delta$ at 1 rad/s.

543 The consistency index, K (Figure S7a) showed a very low statistical dependence on
544 cov-XrL under the studied conditions. Conversely, and regarding polymer concentration,
545 a positive (increasing) statistical correlation was observed, with K growing almost
546 linearly with this parameter and hence, the highest values of K were found at high CTS
547 concentrations. These results may be explained taking into account that, the structural
548 network of hydrogels became more compact as CTS concentration increased due to the
549 increase in hydrogen bond formation [17], far exceeding the influence that the other

550 variable can exert. This is also the trend found for flow index (n) (Figure S7b). Hence, to
551 obtain the lowest values for n , high CTS concentrations should be used.

552 Therefore, it was concluded that, to achieve hydrogels with maximum elastic properties,
553 the use of high CTS concentrations and high degree of cov-XrL were advisable.

554 3.5. Diclofenac Sodium Loaded Formulations from Cross-linked Chitosan- 555 Conjugates and Studies of Drug Release

556 In general terms, and due to the ionizable amino groups present in the polymer
557 backbone, CTS-based hydrogels behave as pH-sensitive DDS, a fact that has been
558 demonstrated in numerous examples such as the release of DOX [8,24], amoxicillin and
559 ibuprofen [23], 5-fluorouracil and diclofenac sodium (DNa) [22] from stabilized CTS-
560 based hydrogels.

561 Values of pH from 5.5 to 7.5 are within the so-called physiological pH figures in human
562 beings; thus, slightly acidic microenvironments are found in mucous membranes and
563 other topical areas. However, maintaining acid-base balance is critical for the survival of
564 living species since cellular processes are highly sensitive to changes in proton
565 concentrations. Although in humans, pH varies within a narrow range (in the blood
566 between pH 7.35 and 7.45), local deviations from the systemic pH are often caused by
567 pathologies, such as cancer, inflammation, infection, ischemia, renal failure or
568 pulmonary disease [44]. Therefore, drug delivery systems capable of releasing the active
569 pharmaceutical ingredient at acidic pH, such as the formulations studied herein, could
570 find significant applications in a wide range of pathologies and locations.

571 Sodium diclofenac (DCNa) is one of the most frequently used non-steroidal anti-
572 inflammatory drugs (NSAID) used to treat pain and inflammatory diseases [45]. Because
573 of the short half-life in plasma (1–2 h) and associated adverse effects [46], it is regarded
574 as an ideal model drug for controlled delivery system [22]. DCNa-loaded hydrogels may
575 have potential applications in the treatment of inflammatory bowel disease (IBD),
576 pathologies of great impact in developed countries [26]. For that use, they may release
577 the drug at the acidic pH typical of inflamed areas and even the small intestine (pH 5-

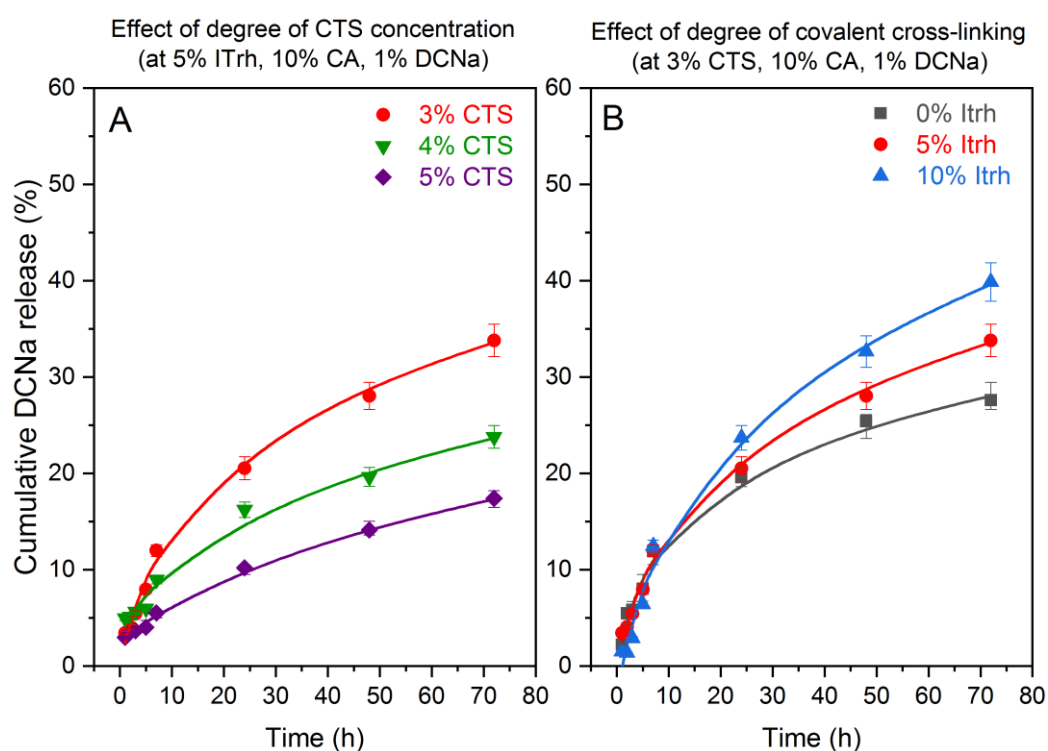
578 7.5) [47–49], and therefore, the release studies of the prepared formulations have been
579 conducted at pH 5.5.

580 As in the study for the rheological properties, ten drug-loaded hydrogel formulations
581 named DCNa-CTS_x-ITrh_y were prepared and are recorded in Table S3. Several examples
582 of formulations of DCNa and CTS have been published, mainly beads, microparticles and
583 hydrogels. For example, the preparation of DCNa-loaded CTS microspheres by double
584 physical emulsification have been described [45] as well as ionically cross-linked
585 DCNa-loaded CTS-based beads was prepared using sodium polyphosphate as a cross-
586 linker. In this case, controlled drug release was confirmed at pH 7.2 and was depended
587 on several formulation factors, such as CTS concentration, drug-polymer ratio and
588 percentage of Tween 80 [50]. The role of silica matrices in DDS has also been explored.
589 DCNa-loaded silica-CTS composites—some of them cross-linked with glutaraldehyde—
590 have been developed to achieve efficient sustained drug-release systems. In this case,
591 the protonated chitosan spheres, were the systems that better controlled the release of
592 DCNa [51]. Regarding gelling systems, Zhang *et al.* prepared DCNa-loaded hydrogels
593 based on carboxymethyl chitosan-*graft*-poly (*N*-isopropyl acrylamide)-glycidyl
594 methacrylate by UV cross-linking. Their findings highlighted that the drug release
595 kinetics depended on pH and temperature. However, the degradability of the networks
596 was not proved for these systems [22]. We have previously investigated the formation
597 of DCNa-loaded ionotropic CTS-based hydrogels in which the drug release and the
598 rheological properties of the systems were strongly dependent on the formulation [17].
599 Unfortunately, the consistency of the prepared matrices ranged from liquid-like to
600 viscoelastic gels. With the aim to improve the physical properties of the materials, in the
601 present study the concentration of CTS has been increased, an additional covalent cross-
602 linking introduced, and the ionic cross-linker replaced by a more hydrophilic molecule.

603 In order to check the release of the DCNa-loaded hydrogels, a calibration curve of the
604 drug was made with DCNa standard solutions at 280 nm [17]. From the samples studied,
605 it was observed that all the hydrogels were able to control the DCNa release for long
606 periods at 37 °C in phosphate buffer at pH 5.5 (Table S3, Figures 8a and 8b). The drug
607 was released in a slow and sustained manner, ranging from 17% to 40% after 72 h. These

608 enhanced retention figures found for the described DCNa formulations were in
609 concordance with the expected results since the anionic drug could be ionically
610 anchored to the cationic CTS-based hydrogels [7].

611 The influence of two factors, CTS concentration and the degree of cov-XrL, on the
612 release profiles was studied. When the role played by CTS concentration on DCNa
613 release was investigated, the other variables, degree of ionic XrL and cov-XrL were set
614 at 10%, and 5% respectively. The results are recorded in Figure 8a.



615

616 **Figure 8.** *In vitro* release profiles of diclofenac sodium (DCNa) from CTS hydrogels in phosphate
617 buffer solution at pH 5.5 at 37 °C. Data were obtained from UV-Vis spectroscopy at 280 nm and
618 reported as mean \pm S.D from three independent experiments. (Fig. 8A) Effect of CTS
619 concentration — from 3% to 5% CTS concentration — in drug release (fixed paraments: degree
620 of covalent cross-linking 5%; degree of ionic cross-linking 10%; DCNa concentration 1%). (Fig. 8B)
621 Effect of degree of covalent cross-linking — from non-cross-linked samples to 10% of cross-linked
622 — in drug release (fixed paraments: CTS concentration 3%; ionic cross-linking 10%; DCNa
623 concentration 1%).

624 It was noted that the greatest changes in DCNa release were found among those
625 formulations with the largest differences in the starting-hydrogels rheological behaviors.
626 For example, for the DCNa-CTS₅-ITrh₅ sample, the DCNa released after 72 h was only the
627 17% of the drug present in the formulation. This could be due to the more developed
628 and complex hydrogel microstructures characteristic of the prepared dispersions with
629 the highest CTS content, as the previous rheological studies had demonstrated. When
630 comparing these findings with the drug release from the DCNa-CTS₃-ITrh₅ sample, it was
631 observed that the percentage of drug delivered by the latter was two-fold the figure of
632 DCNa released from the DCNa-CTS₅-ITrh₅ sample. Consequently, the higher the CTS
633 concentration in the hydrogels, the lower the drug release kinetics. The same trend was
634 reported for disulfide-cross-linked CTS-based hydrogels [7].

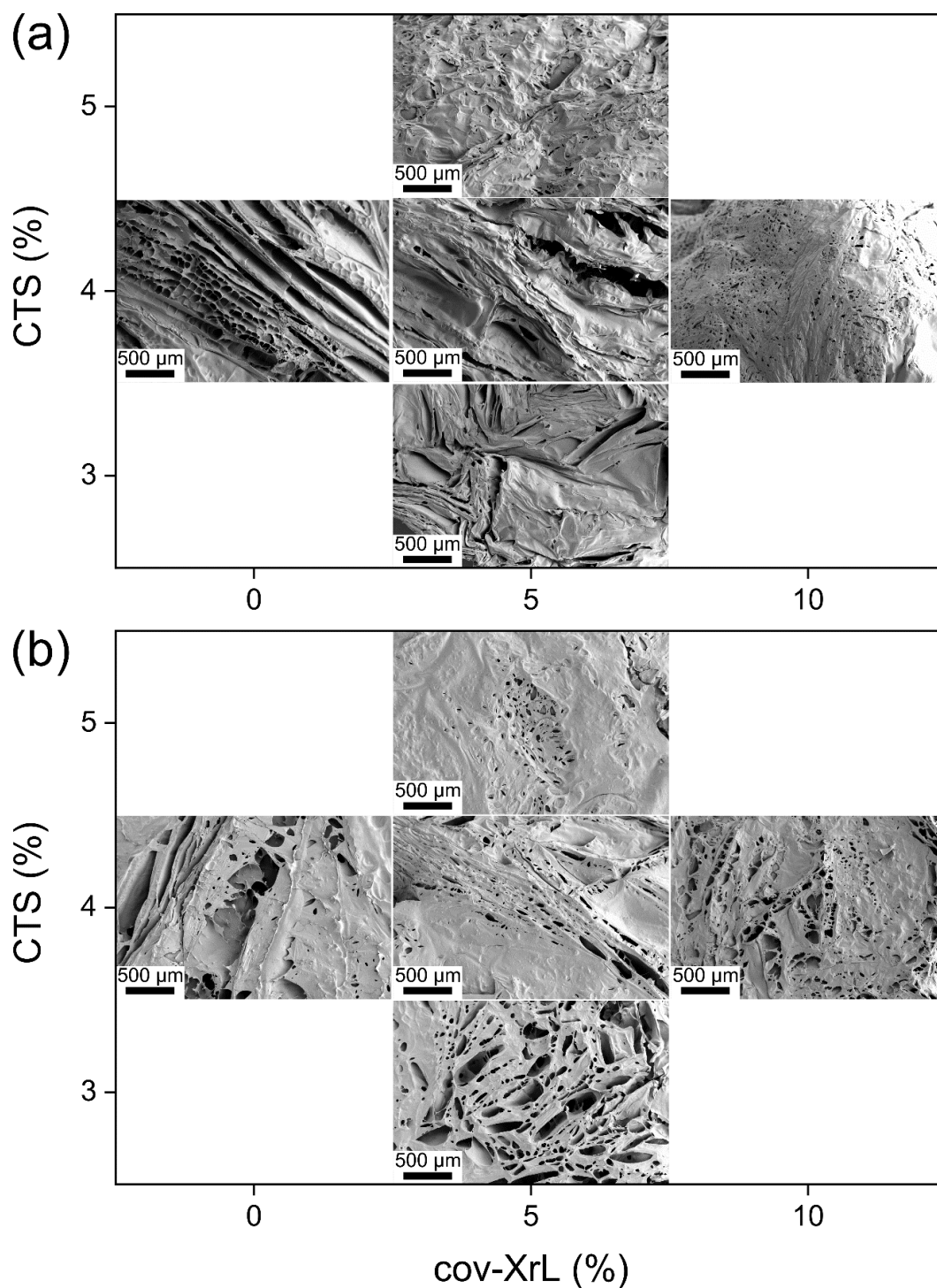
635 Figure 8b shows the release kinetics from selected drug-loaded hydrogels in order to
636 study the impact of cov-XrL on drug release. On the formulations linked to the displayed
637 curves, the degree of ionic XrL was set at 10% for all samples, the percentage of CTS at
638 3% and the concentration of the drug in the formulations at 1%. Although initially
639 surprising, and being the other parameters constant, drug release was enhanced in the
640 most cross-linked systems (cov-XrL: 10%) leading to a boost in drug release. For example,
641 the percentage of DCNa delivered (after 72 h) were 28% and 40% for samples DCNa-
642 CTS₃-ITrt₀ and DCNa-CTS₃-ITrt₁₀, respectively. This assessment related to the influence
643 of cov-XrL in cumulative drug release was accurate for all the formulations studied
644 regardless CTS percentage (Table S3). This trend has also been observed for the release
645 of amoxicillin from CTS-oxidized dextrin hydrogels. Other authors reported that when
646 the cross-linking density of the hydrogels increased, the rate of drug release also
647 augmented. They explained this observation based on the fact that hydrogels with
648 higher cross-linking density would have swelled less, thus causing a higher concentration
649 gradient of the drug. [23] Another hypothesis could be that either the bulky trehalose
650 units between the CTS chains or the volatile solvent used in the preparation of the
651 formulations [52] had behaved as a porogen and may have altered, to some extent, the
652 regular packaging of the CTS in the material. This outcome could have generated
653 interconnected pores that allowed the penetration of water molecules into the
654 matrices, modifying the overall drug release rates due to the generation of drug release

655 channels [53]. Therefore, the higher the degree of cov-XrL, the greater the free volume
656 found in the matrices, and hence, the faster the drug would diffuse into the medium.
657 This assumption was supported by the SEM images found for DCNa-loaded hydrogels at
658 4% of CTS.

659 These findings suggested that the prepared hydrogels can not only act as DDS but can
660 also be used to tune the rate of drug release by changing the degree of cross-linking [8],
661 and/or by modifying the polymer concentration. It is anticipated that the release of
662 non-ionic drugs will show a faster kinetics than those exhibited by the anionic drug
663 DCNa, as it was the case in disulfide-cross-linked CTS-based hydrogels [7].

664 3.6. Scanning Electron Microscopy (SEM) Studies

665 The SEM micrographs displayed in Figures 9a and 9b show the scaffolds of CTS-CA-ITrh
666 and DCNa-CTS-ITrh hydrogels (before and after DCNa loading, respectively) at different
667 CTS concentrations and degrees of cov-XrL. As can be observed in Figure 9a, CTS-CA-ITrh
668 hydrogels prepared with $CTS \leq 4\%$ and $XrL \leq 5\%$ displayed scaffolds with well-defined
669 lamellar structures. At higher CTS contents, such structures tended to disappear in favor
670 of more compact scaffolding. When the degree of cov-XrL reached 10%, matrices
671 containing small pores were found. Similarly to other findings previously reported by us
672 [17], the presence of DCNa caused a change in the morphologies of the hydrogels (Figure
673 9b) and led to more porous microstructures than their non-loaded counterparts. The
674 role of DCNa as a porogen in the hydrogels is hypothesized. For DCNa-CTS-ITrh
675 hydrogels, the lower the percentages of CTS, the greater and larger the number of pores
676 found. These observations are consistent with both the rheological properties of the
677 precursor hydrogels. Evidence of larger number of interconnected pores at low CTS
678 percentages also supports the faster DCNa release found for DCNa-CTS₃-ITrh
679 formulations. It has been demonstrated that interconnected pores may significantly
680 reduce the diffusion length for drug release and the volume fraction of polymer [42].
681 Thus, DCNa-loaded hydrogels prepared with the highest CTS concentration exhibited a
682 developed and complex hydrogel microstructure, responsible for the retention of the
683 anionic drug in the gel-like matrices. The release studies confirmed that the increase in
684 the percentage of CTS decreased the rate of drug release in all the samples studied.



685

686 **Figure 9.** SEM micrographs showing the scaffolds evolution of (a) CTS-CA-ITrh and (b) DCNa-
 687 CTS-ITrh hydrogels at different CTS concentrations and degrees of cov-XrL. For comparison
 688 purpose, all the images were recorded at the same magnification.

689 To sum up, all drug-loaded hydrogels displayed a controlled and steadily DCNa release
 690 at 37 °C with cumulative release figures ranging from 17% to 40% after 72 h. To what

691 extent the drug release occurred was strongly dependent on the composition of the
692 formulation.

693 In despite of the relevant morphological changes observed by SEM in DCNa-loaded and
694 non-loaded hydrogels, it was clear that the ionic interactions established between the
695 anionic drug and the cationic matrices was a relevant parameter regarding drug release.
696 The high percentage of CTS in the systems contributed to a more densely 3D ionic
697 anchoring of DCNa, decelerating the drug release. It is anticipated that the release of
698 non-ionic drugs will show faster kinetics than those exhibited by anionic APIs.

699 4. Conclusions

700 The preparation of a new family of eco-friendly and biodegradable chitosan-based
701 hydrogels have been successfully achieved by means of ionic and covalent cross-linking
702 (ion-XrL and cov-XrL). The novel hydrogels completely disintegrated within 96 h by
703 means of a hydrolysis process mediated by the enzyme trehalase. As far as the authors
704 are aware, this is the first time that a trehalose derivative has been used as a covalent
705 cross-linker in the formation of biodegradable hydrogels, converging the improved
706 physical properties of stable hydrogels with the inherent degradability of ionotropic
707 hydrogels.

708 Through an experimental model design, the influence of two parameters —polymer
709 concentration and degree of cov-XrL— on hydrogel rheological properties was disclosed,
710 being the former the most influential variable. Hydrogels with maximum elastic
711 properties were achieved at the highest CTS concentrations and degrees of cov-XrL.
712 These moduli agreed with the scaffold morphologies found by SEM micrographs in
713 which the hydrogels prepared with lower CTS content and lower degree of cov-XrL
714 showed well-defined lamellar structures, whereas at higher CTS and cov-XrL, such
715 structures evolved to more compact scaffolding.

716 Ten DCNa-containing formulations with different polymer concentration, and degree of
717 cov-XrL were evaluated regarding their release profiles. They displayed well-controlled
718 drug-release patterns that were strongly dependent on the formulation composition,

719 with cumulative drug release varying from 17% to 40% for 72 h under physiological
720 conditions. Systems with improved viscoelastic properties exhibited the lowest rates of
721 drug release. Surprisingly, a boost in drug release was found in those formulations with
722 the highest levels of covalent cross-linking. This trend could be extrapolated to any CTS
723 concentration value.

724 In summary, the preparation method of the CTS-based drug formulations presented
725 herein provides a simple and straightforward pathway to design tailor-made controlled
726 drug delivery systems with improved rheological properties. Their degradability bears
727 real relevance to their potential use in biomedical applications. We anticipate that these
728 systems can be readily adapted to achieve effective encapsulation of other APIs of
729 interest for sustained release.

730 Acknowledgments

731 The authors would like to thank *El Ministerio de Ciencia, Innovación y Universidades*
732 (MICINN) of Spain (Grant MAT2016-77345-C3-2-P), and *La Junta de Andalucía* (Grant
733 P12-FPM-1553) for their financial support.

734 References

- 735 [1] P.M. Favi, R.S. Benson, N.R. Neilsen, R.L. Hammonds, C.C. Bates, C.P. Stephens,
736 M.S. Dhar, Cell proliferation, viability, and in vitro differentiation of equine
737 mesenchymal stem cells seeded on bacterial cellulose hydrogel scaffolds,
738 *Materials Science and Engineering C*. 33 (2013) 1935–1944.
739 doi:10.1016/j.msec.2012.12.100.
- 740 [2] L. Liu, Q. Gao, X. Lu, H. Zhou, In situ forming hydrogels based on chitosan for drug
741 delivery and tissue regeneration, *Asian Journal of Pharmaceutical Sciences*. 11
742 (2016) 673–683. doi:10.1016/j.ajps.2016.07.001.
- 743 [3] N. Annabi, A. Tamayol, J.A. Uquillas, M. Akbari, L.E. Bertassoni, C. Cha, G. Camci-
744 Unal, M.R. Dokmeci, N.A. Peppas, A. Khademhosseini, 25th anniversary article:
745 Rational design and applications of hydrogels in regenerative medicine, *Advanced*

- 746 Materials. 26 (2014) 85–124. doi:10.1002/adma.201303233.
- 747 [4] M.A. Amin, I.T. Abdel-Raheem, Accelerated wound healing and anti-inflammatory
748 effects of physically cross linked polyvinyl alcohol-chitosan hydrogel containing
749 honey bee venom in diabetic rats, Archives of Pharmacal Research. 37 (2014)
750 1016–1031. doi:10.1007/s12272-013-0308-y.
- 751 [5] Y. Liu, S. Hsu, Synthesis and Biomedical Applications of self-healing hydrogels,
752 Frontiers in Chemistry. 6 (2018) 449(1–10). doi:10.3389/fchem.2018.00449.
- 753 [6] N. Bhattarai, J. Gunn, M. Zhang, Chitosan-based hydrogels for controlled,
754 localized drug delivery, Advanced Drug Delivery Reviews. 62 (2010) 83–99.
755 doi:10.1016/j.addr.2009.07.019.
- 756 [7] M.J. Lucero, C. Ferris, C.A. Sanchez-Gutierrez, M.R. Jimenez-Castellanos, M.-V. de-
757 Paz, Novel aqueous chitosan-based dispersions as efficient drug delivery systems
758 for topical use. Rheological, textural and release studies., Carbohydrate Polymers.
759 151 (2016) 692–699. doi:10.1016/j.carbpol.2016.06.006.
- 760 [8] Y. Liang, X. Zhao, P.X. Ma, B. Guo, Y. Du, X. Han, pH-responsive injectable
761 hydrogels with mucosal adhesiveness based on chitosan-grafted-dihydrocaffeic
762 acid and oxidized pullulan for localized drug delivery, Journal of Colloid and
763 Interface Science. 536 (2019) 224–234. doi:10.1016/j.jcis.2018.10.056.
- 764 [9] W.E. Hennink, C.F. van Nostrum, Novel crosslinking methods to design hydrogels,
765 Advanced Drug Delivery Reviews. 64 (2012) 223–236.
766 doi:10.1016/j.addr.2012.09.009.
- 767 [10] S.A. Shah, M. Sohail, M.U. Minhas, Nisar-ur-Rehman, S. Khan, Z. Hussain,
768 Mudassir, A. Mahmood, M. Kousar, A. Mahmood, pH-responsive CAP-co-
769 poly(methacrylic acid)-based hydrogel as an efficient platform for controlled
770 gastrointestinal delivery: fabrication, characterization, in vitro and in vivo toxicity
771 evaluation, Drug Delivery and Translational Research. 9 (2019) 555–577.
772 doi:10.1007/s13346-018-0486-8.
- 773 [11] S.K. Shukla, A.K. Mishra, O. a. Arotiba, B.B. Mamba, Chitosan-based
774 nanomaterials: A state-of-the-art review, International Journal of Biological
775 Macromolecules. 59 (2013) 46–58. doi:10.1016/j.ijbiomac.2013.04.043.

- 776 [12] D. Enescu, C.E. Olteanu, Functionalized Chitosan and Its Use in Pharmaceutical,
777 Biomedical, and Biotechnological Research, Chemical Engineering
778 Communications. 195 (2008) 1269–1291. doi:10.1080/00986440801958808.
- 779 [13] B. Qu, Y. Luo, Chitosan-based hydrogel beads: Preparations, modifications and
780 applications in food and agriculture sectors – A review, International Journal of
781 Biological Macromolecules. 152 (2020) 437–448.
782 doi:10.1016/j.ijbiomac.2020.02.240.
- 783 [14] A. Rafique, K.M. Zia, M. Zuber, S. Tabasum, Chitosan functionalized poly (vinyl
784 alcohol) for prospects biomedical and industrial applications: A review,
785 International Journal of Biological Macromolecules. 87 (2016) 141–154.
786 doi:10.1016/j.ijbiomac.2016.02.035.
- 787 [15] R. Vivek, R. Thangam, V. Nipunbabu, T. Ponraj, S. Kannan, Oxaliplatin-chitosan
788 nanoparticles induced intrinsic apoptotic signaling pathway: A “smart” drug
789 delivery system to breast cancer cell therapy, International Journal of Biological
790 Macromolecules. 65 (2014) 289–297. doi:10.1016/j.ijbiomac.2014.01.054.
- 791 [16] Y. Xu, J. Han, H. Lin, Fabrication and characterization of a self-crosslinking chitosan
792 hydrogel under mild conditions without the use of strong bases, Carbohydrate
793 Polymers. 156 (2017) 372–379. doi:10.1016/j.carbpol.2016.09.046.
- 794 [17] N. Iglesias, E. Galbis, C. Valencia, M.-V. De-Paz, J.A. Galbis, Reversible pH-sensitive
795 chitosan-based hydrogels. Influence of dispersion composition on rheological
796 properties and sustained drug delivery, Polymers. 10 (2018) 1–17.
797 doi:10.3390/polym10040392.
- 798 [18] A. Chenite, C. Chaput, D. Wang, C. Combes, M.. Buschmann, C.. Hoemann, J..
799 Leroux, B.. Atkinson, F. Binette, A. Selmani, Novel injectable neutral solutions of
800 chitosan form biodegradable gels in situ, Biomaterials. 21 (2000) 2155–2161.
801 doi:10.1016/S0142-9612(00)00116-2.
- 802 [19] Y. Xu, C. Zhan, L. Fan, L. Wang, H. Zheng, Preparation of dual crosslinked alginate-
803 chitosan blend gel beads and in vitro controlled release in oral site-specific drug
804 delivery system, International Journal of Pharmaceutics. 336 (2007) 329–337.
805 doi:10.1016/j.ijpharm.2006.12.019.

- 806 [20] C. Ferris, M. Casas, M.J. Lucero, M. V de Paz, M.R. Jimenez-Castellanos, Synthesis
807 and characterization of a novel chitosan-N-acetyl-homocysteine thiolactone
808 polymer using MES buffer., *Carbohydrate Polymers*. 111 (2014) 125–132.
809 doi:10.1016/j.carbpol.2014.03.078.
- 810 [21] M. Dash, F. Chiellini, R.M. Ottenbrite, E. Chiellini, Chitosan - A versatile semi-
811 synthetic polymer in biomedical applications, *Progress in Polymer Science*
812 (Oxford). 36 (2011) 981–1014. doi:10.1016/j.progpolymsci.2011.02.001.
- 813 [22] L. Zhang, L. Wang, B. Guo, P.X. Ma, Cytocompatible injectable carboxymethyl
814 chitosan/N-isopropylacrylamide hydrogels for localized drug delivery,
815 *Carbohydrate Polymers*. 103 (2014) 110–118. doi:10.1016/j.carbpol.2013.12.017.
- 816 [23] J. Qu, X. Zhao, P.X. Ma, B. Guo, Injectable antibacterial conductive hydrogels with
817 dual response to an electric field and pH for localized “smart” drug release, *Acta*
818 *Biomaterialia*. 72 (2018) 55–69. doi:10.1016/j.actbio.2018.03.018.
- 819 [24] J. Qu, X. Zhao, P.X. Ma, B. Guo, pH-responsive self-healing injectable hydrogel
820 based on N-carboxyethyl chitosan for hepatocellular carcinoma therapy, *Acta*
821 *Biomaterialia*. 58 (2017) 168–180. doi:10.1016/j.actbio.2017.06.001.
- 822 [25] R. Dong, Y. Pang, Y. Su, X. Zhu, Supramolecular hydrogels: synthesis, properties
823 and their biomedical applications, *Biomaterials Science*. 3 (2015) 937–954.
824 doi:10.1039/c4bm00448e.
- 825 [26] N. Iglesias, E. Galbis, M.J. Díaz-Blanco, R. Lucas, E. Benito, M.V. De-Paz,
826 Nanostructured Chitosan-based biomaterials for sustained and colon-specific
827 resveratrol release, *International Journal of Molecular Sciences*. 20 (2019) 398 (1–
828 16). doi:10.3390/ijms20020398.
- 829 [27] J. Zhao, X. Zhao, B. Guo, P.X. Ma, Multifunctional interpenetrating polymer
830 network hydrogels based on methacrylated alginate for the delivery of small
831 molecule drugs and sustained release of protein, *Biomacromolecules*. 15 (2014)
832 3246–3252. doi:10.1021/bm5006257.
- 833 [28] J. Berger, M. Reist, J.M. Mayer, O. Felt, N.A. Peppas, R. Gurny, Structure and
834 interactions in covalently and ionically crosslinked chitosan hydrogels for
835 biomedical applications, *European Journal of Pharmaceutics and*

- 836 Biopharmaceutics. 57 (2004) 19–34. doi:10.1016/S0939-6411(03)00161-9.
- 837 [29] L. Zhuang, X. Zhi, B. Du, S. Yuan, Preparation of Elastic and Antibacterial Chitosan-
838 Citric Membranes with High Oxygen Barrier Ability by in Situ Cross-Linking, ACS
839 Omega. 5 (2020) 1086–1097. doi:10.1021/acsomega.9b03206.
- 840 [30] D. Bao, M. Chen, H. Wang, J. Wang, C. Liu, R. Sun, Preparation and
841 characterization of double crosslinked hydrogel films from
842 carboxymethylchitosan and carboxymethylcellulose, Carbohydrate Polymers.
843 110 (2014) 113–120. doi:10.1016/j.carbpol.2014.03.095.
- 844 [31] D. Ailincăi, L. Marin, S. Morariu, M. Mares, A.C. Bostanaru, M. Pinteala, B.C.
845 Simionescu, M. Barboiu, Dual crosslinked iminoboronate-chitosan hydrogels with
846 strong antifungal activity against Candida planktonic yeasts and biofilms,
847 Carbohydrate Polymers. 152 (2016) 306–316. doi:10.1016/j.carbpol.2016.07.007.
- 848 [32] S. Doppalapudi, A. Jain, W. Khan, A.J. Domb, Biodegradable polymers-an
849 overview, Polymers for Advanced Technologies. 25 (2014) 427–435.
850 doi:10.1002/pat.3305.
- 851 [33] T. Sun, Y.S. Zhang, B. Pang, D.C. Hyun, M. Yang, Y. Xia, Engineered nanoparticles
852 for drug delivery in cancer therapy, Angewandte Chemie - International Edition.
853 53 (2014) 12320–12364. doi:10.1002/anie.201403036.
- 854 [34] N. Zhang, H. Zhang, R. Li, Y. Xing, Preparation and adsorption properties of citrate-
855 crosslinked chitosan salt microspheres by microwave assisted method,
856 International Journal of Biological Macromolecules. 152 (2020) 1146–1156.
857 doi:10.1016/j.ijbiomac.2019.10.203.
- 858 [35] A. Sizovs, L. Xue, Z.P. Tolstyka, N.P. Ingle, Y. Wu, M. Cortez, T.M. Reineke,
859 Poly(trehalose): Sugar-Coated Nanocomplexes Promote Stabilization and
860 Effective Polyplex-Mediated siRNA Delivery, Journal of the American Chemical
861 Society. 135 (2013) 15417–15424. doi:10.1021/ja404941p.
- 862 [36] W. Liu, C. Deng, C.R. McLaughlin, P. Fagerholm, N.S. Lagali, B. Heyne, J.C. Scaiano,
863 M.A. Watsky, Y. Kato, R. Munger, N. Shinozaki, F. Li, M. Griffith, Collagen-
864 phosphorylcholine interpenetrating network hydrogels as corneal substitutes,
865 Biomaterials. 30 (2009) 1551–1559. doi:10.1016/j.biomaterials.2008.11.022.

- 866 [37] B. Palma Santana, F. Nedel, C. Perelló Ferrúa, R. Marques e Silva, A. Fernandes da
867 Silva, N.L. Fernando Demarco, Flávio Villarreal Carreño, Comparing different
868 methods to fix and to dehydrate cells on alginate hydrogel scaffolds using
869 scanning electron microscopy, *Microscopy Research and Technique*. 78 (2015)
870 553–561. doi:10.1002/jemt.22508.
- 871 [38] R.H. Schuler, The effect of iodine on the infrared spectra of the alkyl iodides, *The*
872 *Journal of Chemical Physics*. 22 (1954) 947. doi:10.1063/1.1740227.
- 873 [39] S. Iravani, C.S. Fitchett, D.M.R. Georget, Physical characterization of arabinoxylan
874 powder and its hydrogel containing a methyl xanthine, *Carbohydrate Polymers*.
875 85 (2011) 201–207. doi:10.1016/j.carbpol.2011.02.017.
- 876 [40] H.A. Essawy, M.B.M. Ghazy, F.A. El-Hai, M.F. Mohamed, Superabsorbent
877 hydrogels via graft polymerization of acrylic acid from chitosan-cellulose hybrid
878 and their potential in controlled release of soil nutrients, *International Journal of*
879 *Biological Macromolecules*. 89 (2016) 144–151.
880 doi:10.1016/j.ijbiomac.2016.04.071.
- 881 [41] M. Naveed, L. Phil, M. Sohail, M. Hasnat, M.M.F.A. Baig, A.U. Ihsan, M. Shumzaid,
882 M.U. Kakar, T. Mehmood Khan, M.D. Akabar, M.I. Hussain, Q.G. Zhou, Chitosan
883 oligosaccharide (COS): An overview, *International Journal of Biological*
884 *Macromolecules*. 129 (2019) 827–843. doi:10.1016/j.ijbiomac.2019.01.192.
- 885 [42] J. Li, D.J. Mooney, Designing hydrogels for controlled drug delivery, *Nature*
886 *Reviews Materials*. 1 (2016) 16071 (1–38). doi:10.1038/natrevmats.2016.71.
- 887 [43] Y. Hong, H. Song, Y. Gong, Z. Mao, C. Gao, J. Shen, Covalently crosslinked chitosan
888 hydrogel: Properties of in vitro degradation and chondrocyte encapsulation, *Acta*
889 *Biomaterialia*. 3 (2007) 23–31. doi:10.1016/j.actbio.2006.06.007.
- 890 [44] S. Düwel, C. Hundshammer, M. Gersch, B. Feuerecker, K. Steiger, A. Buck, A.
891 Walch, A. Haase, S.J. Glaser, M. Schwaiger, F. Schilling, Imaging of pH in vivo using
892 hyperpolarized ¹³C-labelled zymonic acid, *Nature Communications*. 8 (2017)
893 15126. doi:10.1038/ncomms15126.
- 894 [45] S. Dreve, I. Kacso, A. Popa, O. Raita, F. Dragan, A. Bende, G. Borodi, I. Bratu,
895 Structural investigation of chitosan-based microspheres with some anti-

- 896 inflammatory drugs, *Journal of Molecular Structure*. 997 (2011) 78–86.
897 doi:10.1016/j.molstruc.2011.05.001.
- 898 [46] J. Schwaiger, H. Ferling, U. Mallow, H. Wintermayr, R.D. Negele, Toxic effects of
899 the non-steroidal anti-inflammatory drug diclofenac: Part I: histopathological
900 alterations and bioaccumulation in rainbow trout, *Aquatic Toxicology*. 68 (2004)
901 141–150. doi:https://doi.org/10.1016/j.aquatox.2004.03.014.
- 902 [47] E. Gökbulut, İ. Vural, M. Aşıkoğlu, N. Özdemir, Floating drug delivery system of
903 itraconazole: Formulation, in vitro and in vivo studies, *Journal of Drug Delivery
904 Science and Technology*. 49 (2019) 491–501. doi:10.1016/j.jddst.2018.12.019.
- 905 [48] M. Goud, V. Pandey, Gastroretentive drug delivery system, *International Journal
906 of Pharma and Bio Sciences*. 6 (2016) 158–165.
- 907 [49] R.J. Xavier, D.K. Podolsky, Unravelling the pathogenesis of inflammatory bowel
908 disease, *Nature*. 448 (2007) 427–434. doi:10.1038/nature06005.
- 909 [50] B.S.M. Zadeh, F. Moshtaghi, F. Rahim, A. Akhgari, Preparation and evaluation of
910 sodium diclofenac loaded chitosan controlled release microparticles using
911 factorial design, *International Journal of Drug Development and Research*. 2
912 (2010) 468–475.
- 913 [51] R.B. Kozakevych, Y.M. Bolbukh, V.A. Tertykh, Controlled Release of Diclofenac
914 Sodium from Silica-Chitosan Composites, *World Journal of Nano Science and
915 Engineering*. 3 (2013) 69–78. doi:10.4236/wjnse.2013.33010.
- 916 [52] L. Xinming, C. Yingde, A.W. Lloyd, S. V. Mikhalovsky, S.R. Sandeman, C.A. Howel,
917 L. Liewen, Polymeric hydrogels for novel contact lens-based ophthalmic drug
918 delivery systems: A review, *Contact Lens and Anterior Eye*. 31 (2008) 57–64.
919 doi:10.1016/j.clae.2007.09.002.
- 920 [53] Y. Zhang, X.T. Zhang, Q. Zhang, B. Wang, T. Zhang, Formulation development and
921 evaluation of gastroretentive floating beads with *Brucea javanica* oil using
922 ionotropic gelation technology, *Chinese Journal of Natural Medicines*. 16 (2018)
923 293–301. doi:10.1016/S1875-5364(18)30059-1.

924